The Fourth International Symposium on
GROUND FREEZING
5-7 August 1985
Sapporo, JAPAN

SHEAR STRENGTH ANISOTROPY IN FROZEN SALINE AND FRESHWATER SOILS

Edwin J. CHAMBERLAIN U.S. Army Cold Regions Research and Engineering Laboratory, Hanover, New Hampshire 03755-1290 USA

Abstract

The shear strength anisotropy of frozen freshwater and seawater clay and sand soils was investigated using the direct shear technique. Samples were sheared at angles α of 0, 30, 60 and 90 degrees between the shear and freezing planes.

Because of variations in sample density, there was considerable scatter in the data. This scatter and the relationship of the maximum shear strength to the angle between the shear and freezing planes were accounted for by conducting multiple linear regression analysis on empirical equations relating the test variables to the shear strength.

It was observed that the shear strength generally increased with increasing α, the increase being greater for the sand and for the freshwater condition.

The increase in shear strength for the clay is attributed to the increase in the amount of ice in the shear plane, whereas the shear strength increase in the sand is attributed to the increase in the number of interparticle contacts and the contact stresses. The effect of seawater on the shear strength anisotropy is to reduce the strength of the ice component. This effect is less for the clay than for the sand because less brine is concentrated in the ice component.

Introduction

Frozen freshwater and saline soils commonly have an anisotropic structure resulting from the ice segregation that occurs during freezing. The structure that forms often has the appearance of alternating bands of soil and ice, with linear features aligned normal to the direction of freezing. The soil aggregations and ice lenses can be well defined and highly visible as they frequently are in clays and silts, or they can be hardly distinguishable as they commonly are in sands and gravels. The ice lenses may be clear or they may contain numerous trapped fines. The soil aggregations may contain ice, but the liquid form of water may dominate their structure. When a soil is saturated with seawater prior to freezing, the ice structure may be even more complicated because of the formation of brine pockets within it. Because of this highly preferentially oriented structure, the shear strength of frozen freshwater and saline soils can be anisotropic.

This paper describes a series of laboratory direct shear tests to evaluate the effects of the angle α between the shear and freezing planes on the shear strength of τ_m frozen soil. Two different soils, one a sand and the other a clay, were studied. The major thrust of this research was to understand the effects of seawater on shear strength anisotropy. To do this, both distilled and seawater samples were tested.

Material Description

Two frost-susceptible soils, a fine-grained sand and a clay, were selected for this study. The choice of materials was dictated by the desire to study plastic and non-plastic soils and by the size and shear stress capacity limitations of the available direct shear apparatus. The sand was a well-graded granular material containing numerous fines. The clay was a much finer grained material with a low plasticity. The properties of each of these materials are given in Table 1.

Table 1. Properties of test materials.

Material	Percent passing						Liquid limit (%)	Plasticity index (%)	Uniformity coefficient	Unified soil classification
	2.0 (mm)	0.42 (mm)	0.07 (mm)	0.02 (mm)	0.005 (mm)	0.001 (mm)				
Morin clay	100	100	99	84	52	26	30	9	16	CL
Dartmouth sand	96	68	40	18	6	1	25	NP	29	SM

Direct Shear Apparatus

A standard direct shear (single shear) apparatus was modified to study the shear strength of frozen soils. The apparatus consists of a circular phenolic shear box driven by a variable speed motor. The load is applied through a miniature load cell mounted on a linear ball-bushing-guided load shaft. The horizontal and vertical deformations are monitored by direct current displacement transformers (DCDTs), and are continuously recorded on a strip chart recorder. The shear box (Fig. 1) accommodates a test sample 50 mm in diameter and 58 mm in height. It is made up of four inner rings which contain the test sample and two outer rings through which the shear load is transferred.

The base and cap contain heat exchange chambers through which an ethylene glycol solution is circulated from a refrigerated bath. Radial heat flow is minimized by insulating the shear box and maintaining the ambient room temperature 1°C (2°F)

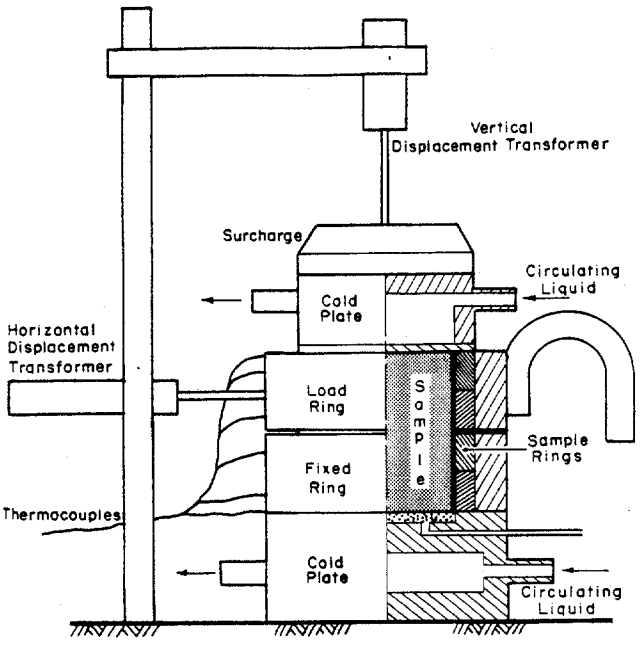

Figure 1. Direct shear test apparatus.

above the desired shear plane temperature. The vertical load on the shear plane is applied through a balance, hangar and weight system common to older types of direct shear devices.

Sample Preparation

The samples were machined to size from larger cylinders of frozen material. These cylinders were obtained by unidirectionally freezing the soil with the appropriate water type freely available during freezing. Details of the freezing equipment have been published elsewhere[2]. Replicate specimens were prepared using both distilled water and seawater as pore fluids.

The test samples were cut from the larger cylinders with a band saw, and the diameter and ends were machined to proper dimensions on a lathe. The samples were prepared with angles α of 0, 30, 60 and 90 degrees. The samples were stored at a room temperature of -10°C prior to testing.

Testing Procedure

The test samples were placed in the direct shear device and allowed to temper at the test temperature for at least two hours. Calibrated miniature thermocouples located on the upper and lower sample surfaces and in the sides of the apparatus just above and below the preferred shear plane were used to monitor the temperatures.

The samples were sheared at shear plane temperatures ranging between 0 and -5°C. The test temperatures were selected to allow the determination of shear strength over a range of temperatures, the shear stress capacity of the apparatus (1200 kPa) limiting the selection of the lowest test temperature.

Once the desired temperature was reached, the sample was sheared at a rate of approximately 0.03 mm/s. Peak stresses usually developed within 5 mm of horizontal deformation. For the tests with the highest shear plane temperatures, the peak streses were not so well defined. In these cases the peak stress was selected as the stress at 5 mm horizontal deformation.

Upon completion of the direct shear tests, each sample was cut into six horizontal slices to determine the water content, salinity and density profiles and the properties in the zone of shearing.

Test Results

A total of 80 direct shear tests were conducted, 24 for each soil type with seawater and 16 for each with distilled water. A standard normal stress of 60 kPa was imposed in most of the tests. Normal stresses of 15 and 180 kPa were also used to evaluate the surcharge effect.

Examples of the resulting shear stress versus deformation curves are shown in Fig. 2. It can be seen that the peak stresses τ_m are well defined and dependent on the α level. In all cases the peak stresses developed at horizontal deformations of 5 mm or lower.

Fig. 3 shows the temperature dependency of the maximum shear stress and the effect of α and N. It can be seen that there is considerable scatter in the data, and that no immediate conclusions can be drawn about the influence of α on τ_m. It will be shown that much of this scatter can be attributed to density variations that occurred during freezing. These plots show clearly, though, that seawater considerably reduces the shear strength of both the sand and clay test materials.

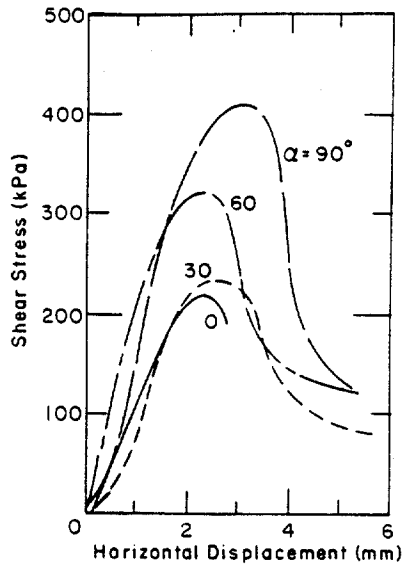

Figure 2. Example of test results for Dartmouth sand frozen with seawater.

Discussion of Results

In order to evaluate the effect of α on τ_m, it was also necessary to identify the effect of density variations from sample to sample and the effect of normal stress N. To do this, simple second degree polynomial curves were selected to relate empirically the sample and test variables

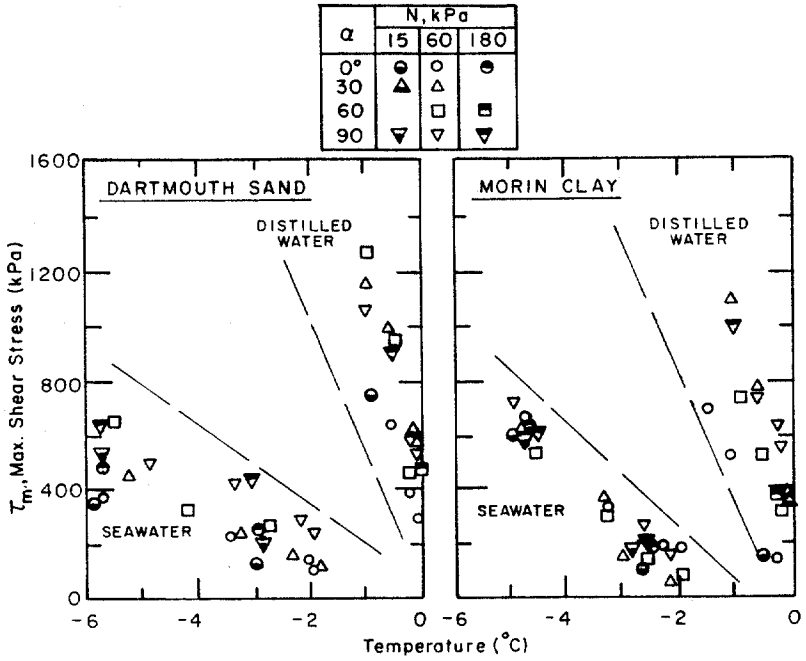

Figure 3. Maximum shear stress versus test temperature for the two test soils.

Table 2. Results of multiple linear regression analysis.

Variable	Morin Clay		Dartmouth Sand	
	Distilled water	Seawater	Distilled water	Seawater
n or e	n	n	e	n
n^2 or e^2	n^2		e^2	
ΔT	ΔT	ΔT	ΔT	ΔT
ΔT^2		ΔT^2	ΔT^2	
α	α	α	α	
α^2	α^2	α^2	α^2	α^2
N		N	N	N
N^2			N^2	
r^2	0.973	0.976	0.987	0.920
S_y	53.1	38.3	48.0	48.0

to the maximum shear strength. These equations generally had the form:

$$\tau_m = a_o + a_1 n + a_2 n^2 + a_3 \Delta T + a_4 \Delta T^2$$

$$+ a_5 \alpha + a_6 \alpha^2 + a_7 N + a_8 N^2$$

The sample porosity n was selected as an index of density. The void ratio e was also used. Because the salinity of the pore water also varied between samples, the difference ΔT between the test temperature and the freezing point of the pore water was used in deference to the actual test temperature.

Multiple linear regression analyses were conducted for each test series. All independent variables had to pass an F-test where the probability that the fit was by chance could not exceed 5%. Table 2 lists the variables accepted for each test series and the resulting correlation coefficients and standard errors.

The resulting fits to the test data were exceptionally good as is shown in Fig. 4 and 5, where τ_m is plotted versus ΔT for each of the four levels of α. These plots were obtained by normalizing the data for each soil-water combination to a common void ratio and normal stress. This was

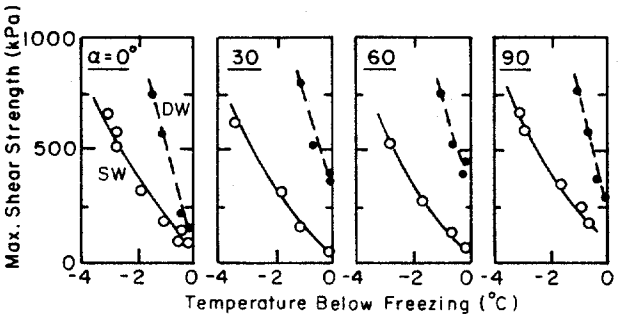

Figure 4. Normalized test results and regression curves for Morin clay (DW = distilled water; SW = seawater; e = 1.25, N = 60 kPa).

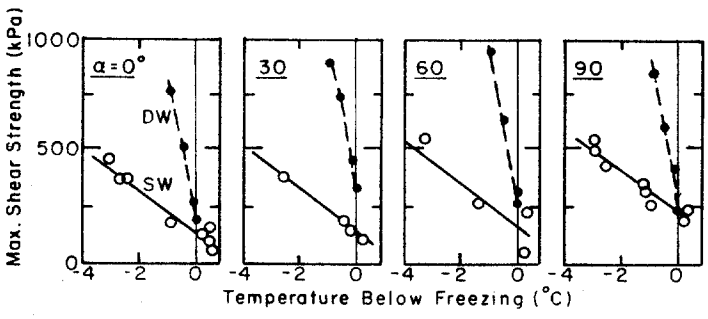

Figure 5. Normalized test results and regression curves for Dartmouth sand (e = 1.0, N = 60 kPa).

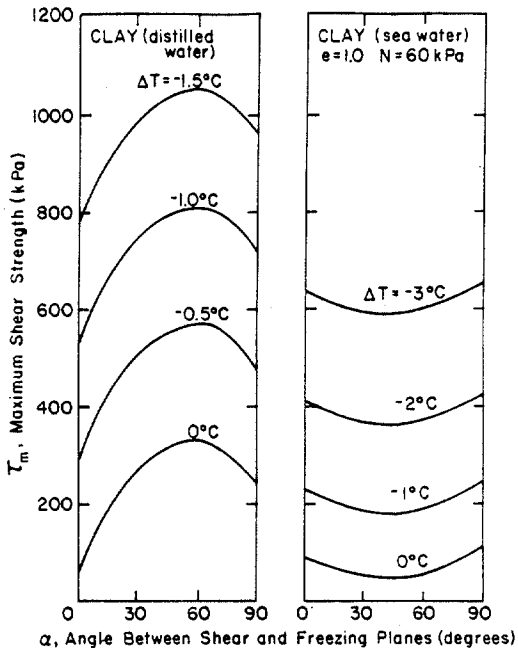

Figure 6. Shear strength anisotropy for Morin clay.

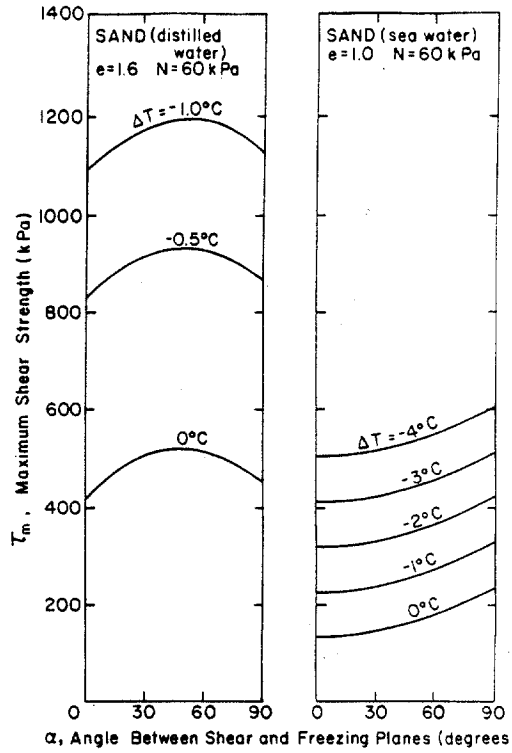

Figure 7. Shear strength anisotrophy for Dartmouth sand.

accomplished by substituting the test α and ΔT values and normalized e and N values in the regression equations and adjusting the resulting estimates of τ_m to have the same percentage error from the regression line as the raw test data.

The resulting data fits show that there is a trend for τ_m to increase with increasing α for all but the clay - seawater combination.

To observe these relationships more closely, the curves in Fig. 6 and 7 were prepared. Here the effect of α on τ_m is clear. The greatest influence is for the clay frozen with distilled water (Fig. 6). In this case, the shear strength is nearly 300 kPa greater when α is 60° than when α is 0°. For the clay - seawater combination, however, there appears to be little influence of α and τ_m, the shear strength being approximately 50 kPa less in the range of α = 30° to 60° than when α = 0°. Since the decrease is of the same magnitude as the standard error for this data set (S_y = 38 kPa), it should not be considered significant.

For the sand - distilled water case (Fig. 7), there is an increase in τ_m of more than 100 kPa occurring at α = 60°. As for the clay - distilled water case, there is a reduction in τ_m as α = 90° is approached. For the sand - seawater combination, the increase in τ_m is also 100 kPa, but the maximum value occurs at α = 90°.

For the clay, the increase in τ_m with increase in α probably results from the increase in the amount of ice in the shear plane. Fig. 8a, b, c and d show thin sections for the frozen clay - distilled water case for α = 0, 30, 60 and 90° respectively. Note (Fig. 8d) that the soil occurs in aggregations or "peds" separated in the plane of freezing by segregated ice. The shear strength is lowest when α = 0° because the shear plane can propagate through nearly a continuous soil layer

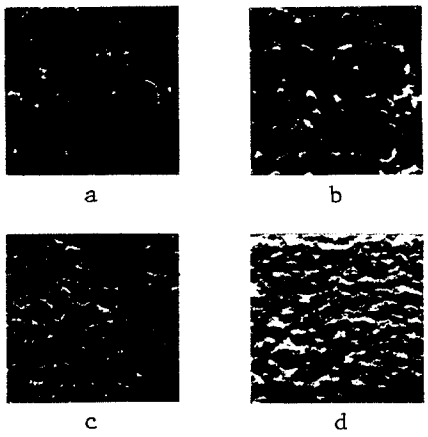

Figure 8. Thin section profiles for Morin clay; a) α = 0°; b) α = 30°; c) α = 60°; and d) α = 90°.

containing large amounts of unfrozen water and small amounts of ice (Fig. 8a). As α increases, the shear plane is forced to pass through more segregated ice, which has greater strength than the soil peds. Why τ_m does not also increase with increasing α for the frozen clay - seawater case is uncertain as the thin sections have an appearance similar to that shown in Fig. 8. It is perhaps due to brine pockets occurring within the ice that cause a reduction in strength in the ice component.

The increase in τ_m with increase in α for the sand is probably the result of increases in the number of interparticle contacts and contact stresses. We were unable to obtain thin sections of the sand to examine the soil-ice structure because of the large particle sizes. However, visual examinations of freshly broken surfaces revealed that the soil-ice structure is quite different in the sand than in the clay as individual or small groups of particles are separated by ice in the sand, whereas larger aggregations of particles separated by ice dominate the structure in the clay. For $\alpha = 0°$, the sand is stronger than the clay because shearing must occur through the ice or at the ice-soil bonds, not through soil aggregations. As α increases in the sand, there is less continuity of ice in the shear plane, and particle interaction and ice bonding cause the increase in τ_m. For the frozen sand - seawater case, the increase in τ_m with increasing α is less dramatic than for the sand - distilled water case, perhaps for the same reason as for the clay - seawater case. Brine pockets within the ice structure cause a reduction in the ice strength.

It should be noted in Figures 4 and 5 that the clay frozen with seawater is stronger than the sand frozen with seawater, even though the sand is denser. The reason for this may be related to the location of the brine excluded during freezing. In the frozen clay-seawater system, the brine can be located within the clay peds, in unfrozen films at the surface of the clay peds or within the ice component. In the frozen sand-seawater case, the brine can be located only in the unfrozen water films adjacent to the soil particles or within the ice. Because of this difference, the volume of brine concentrated in the ice in the frozen sand can be greater, and thus the strength of the ice in the sand can be lower than in the clay.

Summary and Conclusions

The shear strength of ice-bonded freshwater soils is anisotropic, the strength increasing with increasing angle between the shear and freezing planes. The shear strength of soil frozen with seawater is also anisotropic but to a lesser degree. It is the differences in soil-ice-unfrozen water structure that determine the differences in shear strength anisotropy between soil-water types.

The results are important to the design of ice-bonded geotechnical structures. They show that consideration of the relationship of the angle between potential failure surfaces and freezing surfaces can lead to more accurate designs, particularly in freshwater soils. When saline soils are encountered the shear strength anisotropy may also be important, but to a lesser degree.

Since the effect of seawater on the shear strength anisotropy depends on soil type, and probably also on salinity, site-specific direct shear tests need to be conducted for particular projects. Furthermore, because creep is often the cause of failure in frozen ground, the effects of soil-water-ice anisotropy on creep deformation needs yet to be studied.

Aknowledgements

The author wishes to acknowledge the assistance in testing provided by Mssrs. Richard Roberts and Calen Colby and the technical and editorial reviews given by Mssrs. David Cole and Steven Bowen.

References

1) E. Chamberlain 1985 Shear strength in the zone of freezing in saline soils. Proceedings, American Society of Civil Engineers Specialty Conf., ARCTIC '85, p. 566-574.

2) E. Chamberlain 1984 An automated soils freezing test. Proceedings, 2nd National Conference on Microcomputers in Civil Engineering, University of Central Florida, p. 1-5.